Experimental testing of older AASHTO Type II bridge girders with corrosion damage at the ends

Cameron D. Murray, Brittany N. Cranor, Royce W. Floyd, and Jin-Song Pei

In 2013, two bridge girders were selected from separate spans of the eastbound side of the Interstate 244 (I-244) bridge over the Arkansas River in Tulsa, Okla., for testing at the Donald G. Fears Structural Engineering Laboratory at the University of Oklahoma (OU). The bridge was constructed in the late 1960s, and its demolition in 2013 provided an opportunity to test girders that had been in service for decades. The ends of the girders included some corrosion damage that is typical of urban bridges in Oklahoma and may be cause for concern regarding the shear capacity of the girders.

The shear capacity of older bridge girders is of interest because of the deterioration of the end regions and because these girders were designed under an older version of the American Association of State Highway Officials' (AASHO's) *Standard Specifications for Highway Bridges*.[1] The bridge specifications at the time assumed a different critical section for shear than what is used today and also provided a different method of calculating the shear capacity. The design demands from the previous specifications and the deterioration over time combine to create potential strength concerns for shear using updated methods. It is possible not only that the older designs are less conservative for shear but also that the presence of corrosion could reduce the bond of prestressing strands near the member ends. Poor bond can lead to reduced shear and flexural performance due to a reduction in the prestressing force at a given section. In addition to these concerns, there are few studies of bridge girders at the end of their service lives and even fewer that

- This paper discusses the full-scale nondestructive and destructive testing of two 45-year-old AASHTO Type II bridge girders to evaluate shear strength and failure modes.

- The experimental capacity of the girders was compared with the calculated shear capacity based on the original design specifications and updated practice.

- The results of the testing can help determine accurate methods for evaluating shear for in-service bridges, including those with corrosion at the ends.

consider shear capacity specifically. Information on older girders such as these is important as decisions are made about older infrastructure and for properly rating bridges.

This work is a continuation of a previous PCI Convention and National Bridge Conference paper[2] that discussed the girder test results only. This paper contains completed results, including a comparison of tested capacities from both ends of the two bridge girders to the specifications' capacities and demands on the bridge, as well as a discussion of the results. Corrosion of the girder ends was examined as it relates to the performance of the beam from the edge of the discontinuity region (D-region) up to the quarter-span point. Other areas of interest were the behavior of the deck and the diaphragms. The information gained from the testing is intended to help inform rating decisions for bridges constructed with similar girder designs and with similar levels of end deterioration.

Background

Two girders taken from the I-244 bridge over the Arkansas River in Tulsa were tested as part of a project sponsored by the Oklahoma Department of Transportation (ODOT) from 2014 to 2016. The bridge was constructed in the late 1960s and was designed using the AASHO specifications.[1]

At the time these girders were designed, the AASHO specifications[1] took the critical location for shear design as the quarter-span point of the girder. This quarter-point rule meant that the shear at the quarter span of a girder could be taken as the controlling shear demand all the way to the end of the girder. In the American Association of State Highway and Transportation Officials' *AASHTO LRFD Bridge Design Specifications*,[3] the critical section for shear is taken much closer to the girder end. There is some concern that designs from the AASHO specifications may be less conservative in terms of their assumed shear demands toward the ends. Another concern related to the shear capacity of older girders is corrosion. Corrosion at the ends of older girders can lead to reduced bond of the prestressing strands. Reduction in strand bond at the ends of prestressed members can result in reduced shear capacity.

Previous studies on shear in prestressed concrete girders

Several previous studies have considered the residual prestress or flexural performance of prestressed concrete bridges after they have been in service for many years.[4–6] Few studies have considered shear in full-scale prestressed concrete girders. A study performed in Minnesota looked at the shear capacity at both ends of a Type IV girder taken from an older bridge in the state. The goal of these tests was to consider whether previous methods (pre-1980) led to girders that were underdesigned for shear. Despite containing a smaller amount of shear steel than would be required today, the girder carried a greater applied shear than the factored demands in the newer AASHTO LRFD specifications.[7] The Florida Department

of Transportation recovered four Type III AASHTO girders while reconstructing some bridges in the mid-2000s. The girders, which were 30 years old at the time and had shear span–to–depth ratios a/d of 1.2 to 5.4, were tested with a single point load. A common way to identify shear-test locations is a/d because it represents the distance from a discontinuity expressed as a ratio with the depth of the section. The girders were cut from the bridge such that a 28 in. (710 mm) wide section of deck was left atop the girders. Despite their age, the researchers found that the girders did not exhibit reduced capacity compared with current estimates for shear and moment strength. For a/d of 3 or less, bond-shear failures were observed. When a/d was 4, shear-compression failure was observed. For a/d of 5, a flexural failure was observed. Analysis found that modified compression field theory (MCFT) and the provisions of the American Concrete Institute's *Building Code Requirements for Structural Concrete (ACI 318-14) and Commentary (ACI 318R-14)*[8] provided conservative ultimate load values for situations with a/d less than 3 despite the bond-shear failure, which is not explicitly accounted for by these methods.[9,10] In similar work, seven Type II girders from a 42-year-old bridge in Utah were obtained to determine effective prestressing force and ultimate shear capacity. The shear tests were performed at a/d equal to 1.5 using a single point load. The authors found that the AASHTO LRFD specifications' equations were conservative for the failure loads observed during testing.[11]

Prior work at OU has also focused on the shear capacity of aged prestressed concrete girders. In 2008, a 40-year-old AASHTO Type II bridge girder was tested to compare experimental values with values from the 1965 AASHO specifications and the 2004 AASHTO LRFD specifications. The research also compared the values from the AASHO specifications, the AASHTO LRFD specifications, and ACI 318 for shear capacity and demand. The results showed that all three were conservative with regard to shear failure, assuming it occurs at a/d equal to 1.0.[12] This past research is the basis of the continued research performed for ODOT described in this paper. This project examined behavior at additional a/d farther from the girder ends and included a girder with a concrete deck. The girders used in this study exhibited less physical damage prior to testing than the girders used in the previous work. Although most previous work on older Type II girders was performed in D-regions (a/d less than 2.0), this work examines shear performance in the girders between the edge of the D-region and the quarter points.

Girder description

The two girders were selected from the I-244 eastbound bridge over the Arkansas River in Tulsa during a visit to the site in the spring of 2013 before demolition began on the bridge. These two specific girders were chosen to represent two of the four reinforcement configurations used for the AASHTO Type II girders in different spans of the bridge. The girders were named alphabetically based on the various girder designs in the original plans. (Girders with the cross-sec-

tion designs A and C were obtained for this study). The first girder, labeled I244A in this study, was a 30 ft (9.1 m) long AASHTO Type II girder prestressed with six straight ½ in. (12.7 mm) diameter strands and four strands harped at 35% of the length. This girder had been cut from the full bridge in a way that left a section of the 8.5 in. (220 mm) thick deck—with a width roughly equal to that of the top flange—intact. The second girder, labeled I244C in this study, was taken from a different span of the same bridge. I244C was a 46 ft (14.0 m) long AASHTO Type II girder prestressed with ten straight strands and six harped strands (and with the same strand size and harping location as I244A). It was delivered with a roughly 36 in. (910 mm) wide portion of deck intact. The deck was not cut symmetrically about the center of the girder, however, so an additional 10 in. (250 mm) width of deck was cast on the short side to regain section symmetry using a concrete designed to match the strength of cores taken from the deck of I244A. I244C also had partial diaphragms remaining at the center and the ends. Both spans of the I-244 bridge had end and middle diaphragms in service. Both girders were reinforced for shear with double no. 4 (13M) Z bars that were spaced at the following distances:

- 4 in. (100 mm) for the first 12 in. (300 mm) of the girder (from each end)

- 8 in. (200 mm) from 12 in. up to 30% of the girder length (from each end)

- 12 in. for the interior 40% of the length of the girder

Figures 1 and **2** show the cross sections of the girders as designed and the delivered sections including the deck, respectively. Both girders had a 6.5 in. (160 mm) thick original deck with a 2 in. (50 mm) concrete deck overlay.

The two girders each had mild to moderate corrosion damage at one end. **Figure 3** shows the worst example of the damage (on I244A), with exposed strands and visible section loss. I244C did not have such significant corrosion in terms of visible deterioration of the strands, but some initial cracking around the strands was present due to corrosion. The opposite end of each girder had relatively little corrosion. Samples of the most corroded strands were removed from the I244A girder after testing was completed. Evidence of corrosion (for example, rust and pitting) was visible on these strand samples for up to 8 in. (200 mm) from the strand end. Strand samples were not removed from I244C because this girder was slated for repair and rehabilitation as part of an associated project, but strands exposed by spalling during testing exhibited visible corrosion extending a similar distance into the beam.

Material properties

Concrete properties

Cores were taken from the deck and web of both girders after testing was completed. Care was taken to avoid areas of the girders damaged by the shear tests. Core strengths were adjusted using ACI 214.4 *Guide for Obtaining Cores and Interpreting Compressive Strength Results*[13] to account for differences in the core sizes from standard dimensions. The number of cores that could be retrieved from I244C was limited because the girder was needed for future research. Six cores were taken at different locations along the length and depth of the web of I244A for compressive strength testing. The average compressive strength for these cores was 6570 psi (45.3 MPa), which was close to the specified compressive strength of 6000 psi (41.4 MPa) from the original plans. Six cores were taken from the deck in the center section of I244A. The average compressive strength of all deck cores
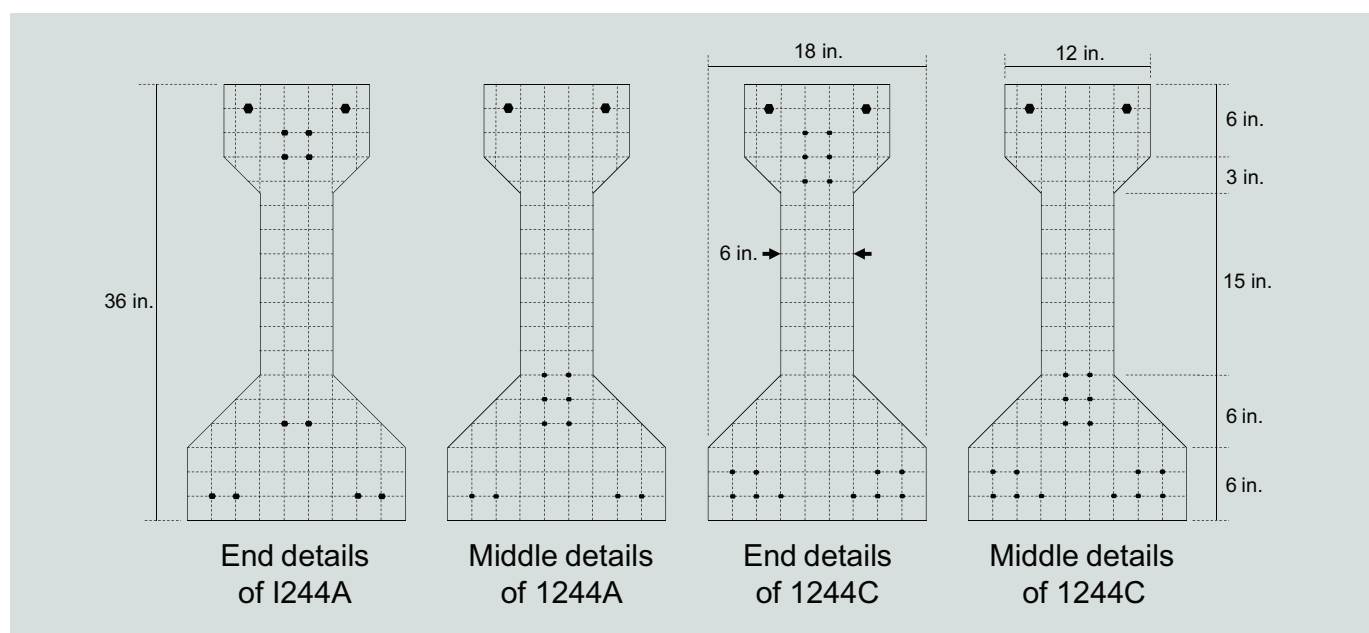
Figure 1. Details of I244A and I244C with an overlaid 2 in. (50 mm) grid to show the dimensions more clearly. Note: 1 in. = 25.4 mm.
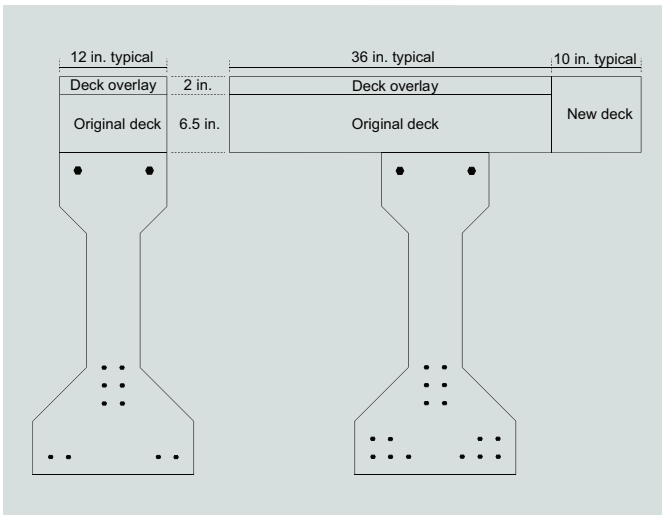
Figure 2. Deck details as tested for I244A (left) and I244C (right). Note: 1 in. = 25.4 mm.

Figure 3. Corrosion at tested end for test A1.

(excluding a core containing reinforcing bar) was 7840 psi (54.1 MPa). The modulus of elasticity of the I244A concrete was determined from seven cores taken from the girder web using the methods of ASTM C469, *Standard Test Method for Static Modulus of Elasticity and Poisson's Ratio of Concrete in Compression*.[14]

The average modulus of elasticity of the I244A concrete was 4750 ksi (32.8 GPa). The estimated modulus of elasticity using Eq. (C5.4.2.4-1) in the AASHTO LRFD specifications[3] was 4665 ksi (32.2 GPa). The measured modulus of elasticity is greater than the predicted modulus of elasticity (by 1.8%), which indicates that the estimate is appropriate. No values for modulus of elasticity for the deck of I244A were recorded because the available deck was too small and congested with reinforcement to retrieve a large enough core.

The average compressive strength of the cores taken from the I244C girder web was 7180 psi (49.5 MPa), and the average compressive strength for the cores taken from the deck was 6060 psi (41.8 MPa). One deck core appeared to have low compressive strength relative to the other breaks. If this break value is not considered, the average compressive strength of the deck cores was 6690 psi (46.1 MPa). All usable cylinders from the I244C web were used for determining the compressive strength. However, only the web cores were used to test for modulus of elasticity because the deck cores were not tall enough. Based on the AASHTO LRFD specifications' modulus of elasticity correlation, the web modulus was 4875 ksi (33.6 GPa) and the deck modulus was 4480 ksi (30.9 GPa).

As mentioned, I244C was delivered to the Donald G. Fears Structural Engineering Lab at OU with an unsymmetrical section of deck on top and an additional 10 in. (250 mm) of deck width was added before testing (Fig. 2). The concrete was designed to provide similar properties to the existing deck concrete (based on I244A strengths). Interface steel was attached to the existing deck at a similar spacing to the transverse deck reinforcement using structural epoxy. The

surface of the existing concrete was roughened with a rotary hammer to improve bond with the new concrete. The 28-day concrete compressive strength from the deck addition was 6350 psi (43.8 MPa), similar to cores taken from I244A and the original deck of I244C.

Steel properties

Two prestressing strand samples taken from the center section of I244A were tested for tensile strength and modulus of elasticity using ASTM A1061, *Standard Test Methods for Testing Multi-Wire Steel Prestressing Strand*.[15] The average modulus of elasticity of the strands was 26,350 ksi (181.7 GPa). The average tensile strength of the strands was 283 ksi (1950 MPa), confirming that the strands were Grade 270 (1860 MPa), as specified in the original plans. Two samples of mild reinforcing steel from the shear stirrups in I244A and from the reinforcement in the diaphragm (removed prior to testing) were tested for yield stress, ultimate strength, and modulus of elasticity. The average yield strength, modulus of elasticity, and ultimate strength for the shear stirrups were 54.8, 32,750, and 87.9 ksi (378 MPa, 226 GPa, and 606 MPa), respectively. For the diaphragm reinforcement, these values were 51.1, 27,500, and 84.2 ksi (352 MPa, 190 GPa, and 581 MPa). These properties confirm that the mild steel reinforcement was most likely Grade 40 (280 MPa), which was assumed during preliminary analysis of the girders based on the original plans.

Description of testing

Nondestructive tests

To evaluate the residual stiffness of I244A, 17 elastic flexural tests up to a point load of 15 kip (67 kN) were performed at varying load points and support locations. Deflection was measured along the length of the beam using linear variable displacement transducers (LVDTs) centered on the girder soffit for all locations except the centerline, where LVDTs were

placed on each side of the bottom flange of the girder. Tensile strain due to bending was measured using strain gauges attached to the bottom flange of the girder.

Destructive tests

Previous work at OU by Martin et al.[12] was continued in the destructive shear tests. The *a/d* for this study was continued from the starting point of 1.0 used in the previous study. Both girders were tested once at each end: I244A at *a/d* of 2.0 and 2.5 and I244C at *a/d* of 3.0 and 3.83 (quarter point). The girders were supported at one end and at a location that left the opposite end overhanging such that it would not be damaged or influence the test of the opposite end. Neoprene bearing pads were used at the supports to match field conditions observed during a visit to the bridge. The bearing pads were 6 in. (150 mm) wide, 18 in. (460 mm) long, and approximately 1 in. thick (25 mm). The pads were placed as close to the ends as possible while still allowing full bearing along the bottom of the girder end.

A single point load was applied through a steel plate using a hydraulic actuator. The applied force was measured using a 400 kip (1780 kN) capacity load cell. Surface strain was measured at several locations during both tests using electrical resistance strain gauges and full-bridge strain transducers. Deflection under the load point was measured using wire potentiometers, and strand slip was monitored using LVDTs on selected strands at the tested end of the girders. A grid was drawn on the girders to assist in tracking the locations of cracks during testing. A 3 in. (75 mm) grid was used for girder A, while a 6 in. (150 mm) grid was used for girder C. Deflection of the bearing pads was monitored with two LVDTs on each end. In general, load was applied to the girders in 10 kip (44 kN) increments until initial cracking was observed. From this point on, the load was applied in 5 kip (22 kN) increments. Cracks were marked as they occurred, and load was increased incrementally until failure.

Testing results

Nondestructive tests

Flexural stiffness testing at the midpoint of the girder resulted in an average stiffness of 388.2×10^6 kip-in.^{2} (1.114×10^6 kN-m^2) for I244A. This value was derived from the slope of the load-deflection diagrams from the elastic flexural tests up to the applied force of 15 kip (67 kN). Using the measured flexural stiffness and the calculated transformed section moment of inertia (104,949 in.^{4} [4.3683×10^6 mm^4]) implies a modulus of elasticity of 3700 ksi (25.5 GPa), which is 78% of the modulus of elasticity of cores taken from the girder (4750 ksi [32.8 GPa]). Deflection measurements using this method are very small compared with the size of the girder; therefore, minute errors can influence the final result. The girder soffit was uneven, which resulted in variations in the support conditions, some of which were of the same magnitude as the measured deflections. The deflections, including

settlement at the supports, were measured with the best instruments available. If this method is used in the future, however, care should be taken to reduce the effects of these sources of error in deflection measurement.

To limit damage to the girders before the destructive tests, cracking moment was measured during the destructive tests. The recorded cracking moments proved difficult to reconcile with the estimated prestressing force due to the difficulty of accounting for interaction of stresses caused by moment, shear, and the draped strands. Residual prestressing forces calculated using the measured cracking moments from the test of each end were 97% and 105% of the initial values. By comparison, the expected prestressing force based on the AASHTO LRFD specifications[3] was approximately 80% of the initial prestressing force. Cracking moments were not measured in I244C due to these difficulties.

Destructive tests

The first test of I244A (A1) was performed at an *a/d* of 2.5 with a span length of 18.75 ft (5.72 m). Initial cracking, which was due to flexure, occurred at an applied shear of 104 kip (463 kN) directly under the load point (applied moment = 753 kip-ft [1021 kN-m]). The first shear crack was a web-shear crack 4.5 ft (1.44 m) away from the load point toward the near support and occurred at an applied shear of 138 kip (614 kN). As the load was increased, several shear cracks began at the bottom flange. At an applied shear of 157 kip (698 kN), the bottom four strands slipped, leading to a loss of load-carrying capacity. Slip was measured for six of the strands before failure, which was possibly influenced by the corrosion (Fig. 3) present at the girder end. Shear was increased to a maximum of 160 kip (712 kN), at which point the deck overlay delaminated. The cracking pattern for this test is shown in **Fig. 4**. Initial flexure cracking occurred near the load point. Flexure-shear and web-shear cracks occurred between the load point and near support (Fig. 4). The failure mode for test A1 can be characterized as bond shear/flexure because strand slip reduced the capacity of the section and ultimately led to a shear failure that included flange crushing.[16] Because *a/d* was less than 3.0, a bond-shear failure was expected based on work by Ross, Ansley, and Hamilton.[9] The strand slip reduced the available tie force and contributed to the shear-cracking and shear-failure mechanism. The deflection measurements for test A1 were lost due to a malfunction of the wire potentiometers, so load-versus-deflection data were not available for this test. **Figure 5** shows a photo of the failure.

The second test of I244A (A2) was performed at an *a/d* of 2.0 with a span length of 19 ft (5.8 m). Initial cracking, due to flexure, occurred directly under the load point at an applied shear of 133 kip (592 kN), corresponding to an applied moment of approximately 756 kip-ft (1025 kN-m). The first shear crack was observed in the web and the bottom flange roughly 1 ft (0.3 m) away from the support at a shear of 158 kip (703 kN). Shear was increased to a maximum value
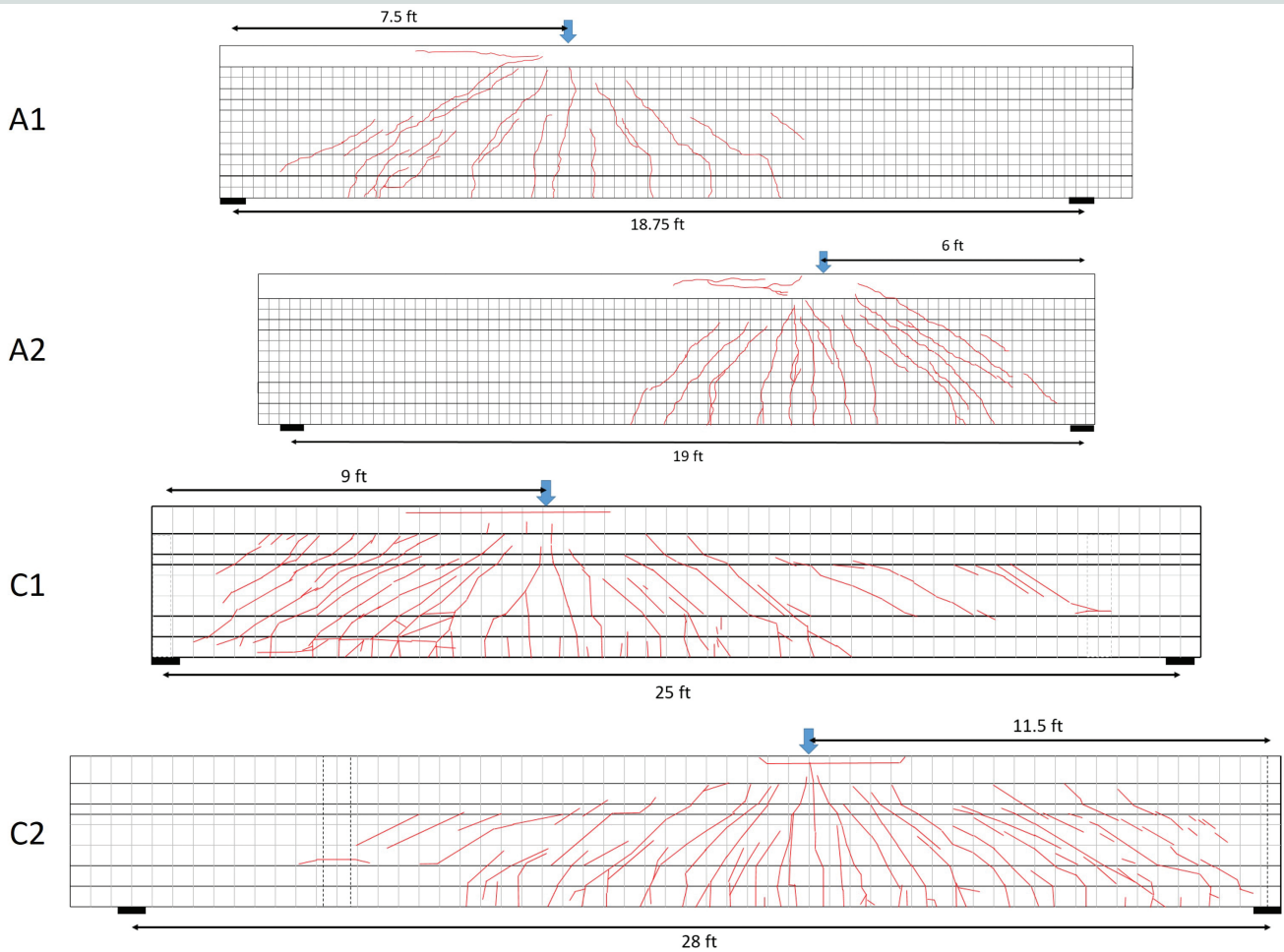
Figure 4. Cracking patterns for all tests: 3 in. (75 mm) grid shown for A1 and A2, and 6 in. (150 mm) grid shown for C1 and C2. Note: 1 ft = 0.305 m.

of 203 kip (903 kN), corresponding to an applied moment of 1151 kip-ft (1561 kN-m), at which point there was a sudden failure corresponding to delamination of the deck overlay and rupture of multiple prestressing strands. The strands ruptured approximately 1 ft away from the load point in the direction of the longer side of the span. The cracking pattern is shown in Fig. 4, and a photo of the final failure is shown in Fig. 5. **Figure 6** shows the load-deflection plot for test A2. This plot indicates a period of constant load and yielding at the maximum load, which is generally indicative of the ductility associated with a flexural failure. This failure type was confirmed by crushing of the extreme compression fiber and fracture of at least two of the bottom-layer prestressing strands. Figure 6 includes markers for when initial flexural cracking and shear cracking were observed, as well as the ultimate load. A change in slope precedes the first visually identified crack.

The first test of I244C (C1) was performed at an *a/d* of 3.0 with a span length of 25 ft (7.6 m). At an applied shear of 55 kip (245 kN), spalling was observed at the end nearest the load point above the neoprene bearing pad. The strands at that end of I244C were corroded similarly to that described for I244A. The bearing force caused the preexisting corro-

sion-induced cracks at this end to open and for concrete to spall off of the bottom flange (**Fig. 7**). At this point, the test had to be stopped so the LVDTs on the strands at that end of the girder could be repositioned. When the test was resumed, spalling mostly ceased and web-shear cracks were observed at an applied shear of 101 kip (449 kN) at the web-top flange interface. Flexural cracking under the load was observed at a shear of 117 kip (520 kN).

This test was stopped at a point load of 195 kip (867 kN) before continuing the load to failure because of a data acquisition error. As load increased beyond this point, several shear cracks began to align themselves with the strands in the bottom flange, indicating a possible bond-shear issue. The test had to be stopped and the load removed when the hydraulic actuator ran out of stroke. Load was reapplied up to failure after an additional spacer was added. Once a maximum shear of 204 kip (907 kN) was reached, the shear cracks at the bottom flange became wider and the strands slipped, leading to additional deflection and delamination and crushing of the deck overlay. Based on published recommendations for classifying bond failures,[16] this failure could be described as due to flexure bond. However, the delamination of the deck during
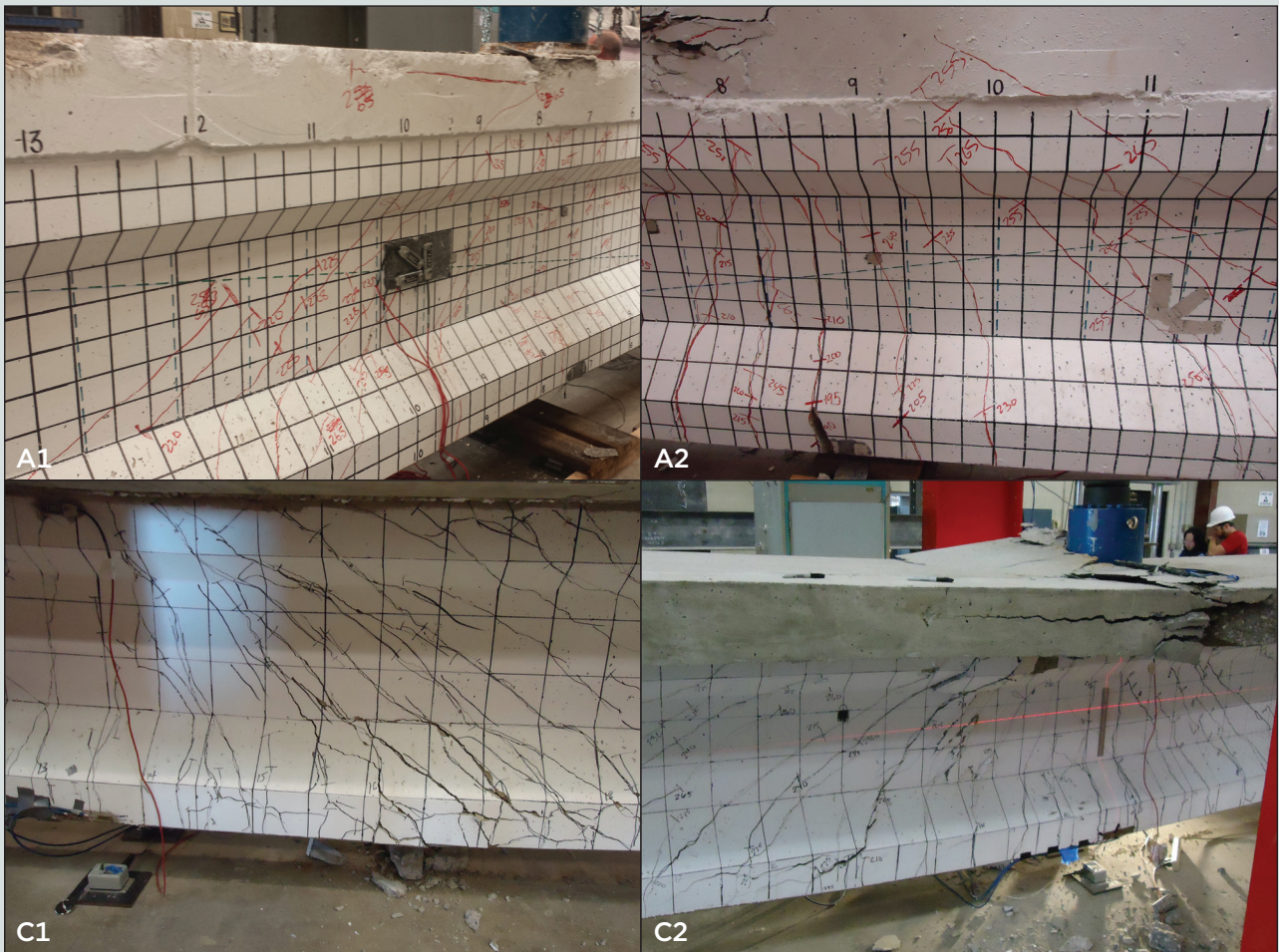
Figure 5. Failure photos from each test.

these girder tests makes classifying the failure difficult. Deck delamination may not be interpreted as flange crushing because the interface between the overlay and original concrete deck had less strength than the original deck concrete and thus failed prior to reaching the compressive capacity of the deck. Figure 4 shows the cracking pattern for test C1. Horizontal cracking along the bottom flange is visible, indicating loss of bond between the strands and concrete. Figure 6 shows a load-deflection curve for test C1. This figure shows the last two sets of data (tests B and C). The first, when the support deflections were disturbed by spalling concrete (test A), is not included. The stiffness in test B was slightly less than in test A due to initial cracking when the first test was stopped. Strand slip was measured in five of the instrumented strands during this test. Cracking entered the transfer length and caused this slip, leading to a decreased shear resistance.

The second test of I244C (C2) was performed at an *a/d* of 3.83, corresponding to a quarter of the original span length. In the 1965 AASHO specifications, this point would have been taken as the critical section for shear. However, this far into the span, moment was expected to control the failure based on the assumed material properties. The test span was increased

to 28 ft (8.5 m) to increase the shear demand on the short side of the span. The first observed cracks were web-shear cracks approximately 2 ft (0.6 m) from the supports at an applied shear of 88 kip (391 kN), followed by flexural cracking at a shear of 94 kip (418 kN) (corresponding to a moment of 1074 kip-ft [1456 kN-m]). As load was increased, some shear cracks entered the bottom flange and oriented themselves horizontally along the level of the strands (indicating potential loss of bond). Figure 4 shows an overview of the cracking from test C2. Shear was increased to 179 kip (796 kN), at which point test A was stopped due to a leak in the hydraulic actuator. Load was removed from the girder until the hydraulic system could be topped up with fluid. After the hydraulics were corrected, load was applied continuously until ultimate failure occurred at a shear of 176 kip (783 kN) in test B.

As in previous tests, the girder failed when the forces in the deck overlay were too large, causing delamination and crushing of the deck overlay. The compressive forces during this test were so large that the top flange crushed and compression steel in the top flange and the deck buckled (Fig. 5). This failure type could be described as compression shear or a flexural failure. Compression shear is caused by shear cracks entering
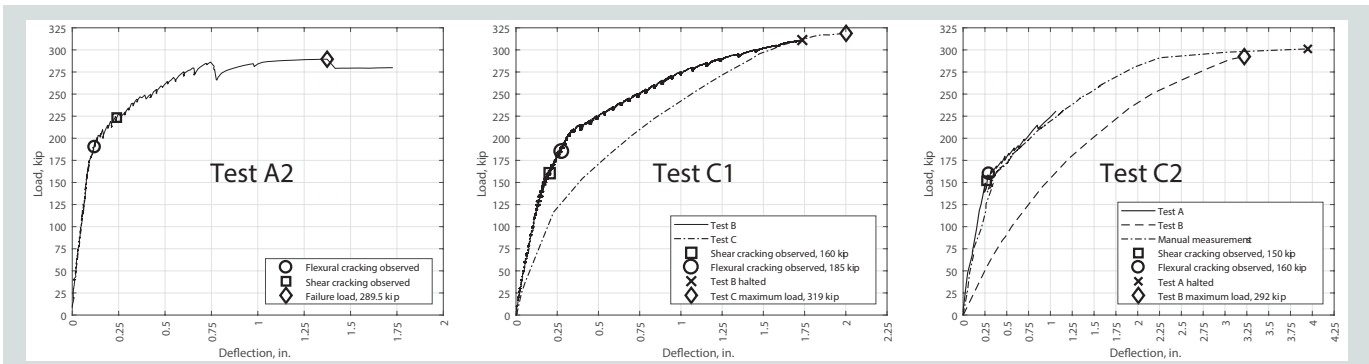
Figure 6. Deflection versus load for tests A2, C1, and C2. Note: 1 in. = 25.4 mm; 1 kip = 4.448 kN.

the compression flange followed by a compression failure. This failure type is common for this *a*/*d*.[9] Figure 6 shows the load-deflection curves for both iterations of test C2 (tests A and B). The wire potentiometers began to yield unreliable data at a load of approximately 230 kip (1023 kN) during test A, so manual measurements are shown instead of the potentiometer data past this point. After initial cracking, there was an increase in deflection of 3.75 in. (95.3 mm) and many additional cracks appeared, indicating some ductility. Some strand slip was measured in four of the bottom strands in the girder during this test. Despite this slip, the compression steel in both the deck and top flange buckled at failure.

A summary of the four girder tests is shown in **Table 1**. A common failure mechanism in all tests was the delamination of the deck overlay atop the deck. When interface shear forces at the surface between the original deck and the sacrificial deck overlay became too great, the bond here failed, leading to failure of the entire section. Therefore, the deck overlay was always the limiting factor for the overall capacity of the girders. These failures likely occurred at a lower load than if the deck had a monolithic wearing surface rather than a deck overlay, potentially skewing the observed shear behavior. However, the deck overlay appeared to be in addition to the original slab and a smaller thickness would have been used in the original design.

Discussion of results

The goal of the full-scale testing was to evaluate the residual performance of the girders compared with current demands and expected capacities. In addition, specific attention was focused on the effects of corrosion at the ends, shear behavior, and the composite deck. Partial diaphragms were left on the girders but appeared to have negligible effect on the shear behavior. Because there are few examples of full-scale tests of older bridge girders in shear, this discussion can add to the limited literature on girders constructed during the same time period.

Experimental capacities compared with design equations

Results from the four girder tests were compared with the ACI 318 shear method (ACI),[8] the AASHTO LRFD spec-

Figure 7. Spalling under load during test C1 initiated by cracking caused by corrosion.

ifications' simplified procedure (AASHTO-SIMP), the AASHTO LRFD specifications' MCFT procedure using beta-theta equations (MCFT-EQN), the AASHTO LRFD specifications' MCFT procedure using beta-theta tables (MCFT-TAB),[3] and the 1965 AASHO specifications procedure (1965-STD).[1] For these comparisons, the estimated prestress losses were calculated using the AASHTO LRFD specifications' refined method and the measured concrete compressive strengths were used. **Figure 8** shows the calculated capacities for each reported method compared with experimental capacities for all tests. All calculated capacities are nominal; no strength reduction factors are included. The equations compared here do not take into account D-region behavior, which may affect their accuracy—especially for tests A1 and A2, which were performed closer to D-regions. The horizontal line in Fig. 8 indicates the applied shear at failure for each test. The shear at the nominal moment capacity M_n is included to show how it compared with the applied and computed shear capacities.

Figure 8 shows that the experimental shear capacity was generally greater than the capacity calculated by the MCFT-EQN and MCFT-TAB methods at each location tested. In the case of the MCFT-EQN method, the experimental capacity was greater than the predicted capacity by a factor

Table 1. Summary of test data

	Teset A1	Test A2	Test C1	Test C2
a/d	2.5	2.0	3.0	3.83
Span, ft	18.75	19	25	28
$P_{cracking}$, kip	170	190	160	150
$V_{cracking}$, kip	104	133	101	88
$M_{cracking}$, kip-ft	753	756	906	1007
P_{slip}, kip	255	n/a	250	n/a
V_{slip}, kip	157	n/a	159	n/a
M_{slip}, kip-ft	1129	n/a	1411	n/a
P_{max}, kip	260	290	318	301
V_{max}, kip	160	203	204	179
M_{max}, kip-ft	1151	1151	1800	2021
Failure mode	Bond (shear/flexure)	Flexural (strand rupture)	Bond shear	Compression shear (flexural shear)

Note: a/d = shear span–to–depth ratio; $M_{cracking}$ = applied moment at cracking load; M_{max} = applied moment at maximum load; M_{slip} = applied moment at first measured strand slip; n/a = not applicable; $P_{cracking}$ = cracking load; P_{max} = maximum load; P_{slip} = load at first measured strand slip; $V_{cracking}$ = applied shear at cracking load; V_{max} = applied shear at maximum load; V_{slip} = applied shear at first measured strand slip. 1 ft = 0.305 m; 1 kip = 4.448 kN; 1 kip-ft = 1.356 kN-m.

(experimental capacity divided by predicted capacity) of 1.19 to 1.49. The MCFT-TAB method was accurate for the configurations tested, with factors between 0.97 and 1.3. The MCFT-EQN was developed as a simplification of the MCFT-TAB method and was reported by its developers to be more conservative.[17] Both of these methods predict lower concrete contributions to shear strength than the other methods. The other shear equations occasionally overpredicted shear capacities.

For test A1 (bond-shear failure), the 1965-STD, ACI, and AASHTO-SIMP methods all overpredicted capacity (with experimental capacity–to–predicted capacity factors of 0.83, 0.88, and 0.74, respectively). In this case, the capacity of the section was estimated conservatively by strain compatibility for a flexural failure, even though the actual failure mechanism was when bond was lost due to shear cracking. Alternatively, the ACI and AASHTO-SIMP shear equations predicted a greater-than-measured capacity. Some of the inaccuracies of the shear-capacity methods may be due to D-region behavior not accounted for in these methods. Test A1 was performed at an a/d of 2.5. During test A2, prestressing strands near the load point ruptured, indicating a flexural failure. The flexural capacity of the section based on strain compatibility was exceeded during the test. The extent of shear cracking indicates that the girder maintained adequate ductility and load-carrying ability during the test. At the failure load, all shear-capacity calculations were exceeded by the applied shear except AASHTO-SIMP, which exceeded the experimental capacity by 4.6 kip (21 kN).

Test C1 resulted in a bond-shear failure with shear cracks entering the zone of prestressing force transfer and reducing the capacity of the section. The experimental capacity exceeded predictions calculated by current methods, with the exception of AASHTO-SIMP. The ratio of experimental capacity to predicted capacity for AASHTO-SIMP was 0.9 for test C1. The flexural capacity was not reached in this case, so the overpredicted shear capacity of the AASHTO-SIMP would be a governing value for this location. Alternatively, if MCFT were used to estimate the shear capacity, the predicted section capacity would be exceeded by the experimental value (experimental capacity to predicted capacity factors of 1.25 for MCFT-EQN and 1.15 for MCFT-TAB). Test C2 was performed at the quarter point, the critical location for shear per the 1965 AASHO specifications. In this case, the applied load exceeded the flexural capacity as calculated using strain compatibility. The experimental capacity exceeded values calculated using current equations with the exception of ACI and AASHTO-SIMP, which produced experimental capacity–to–predicted capacity ratios of 0.94 and 0.77, respectively.

Table 2 summarizes the experimental capacity–to–predicted capacity ratios. Not considering test A2, which can be characterized as a flexural failure, the ratios were averaged to determine how accurate each method was, in general, for the configurations tested. A coefficient of variation (COV) is given to indicate the variability of each method. This is a limited sample size (three tests) to indicate a COV, and it is not included here to represent the general variability of the
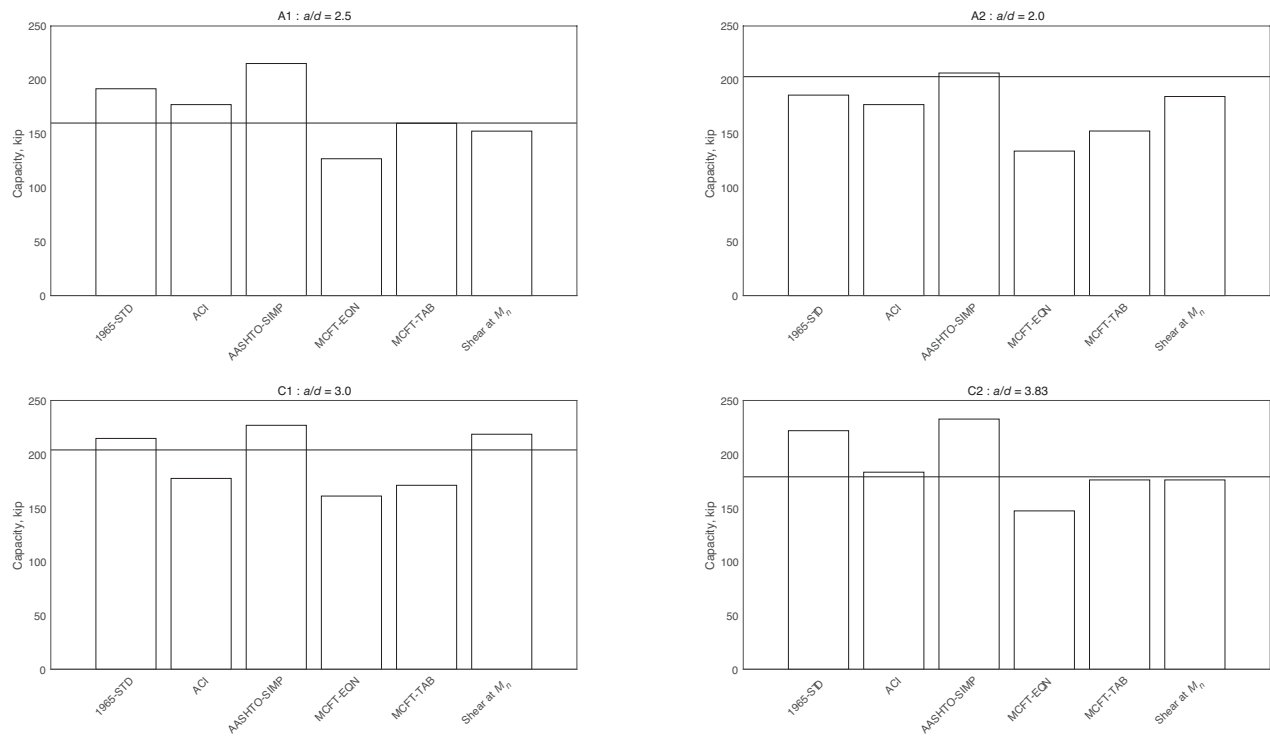
Figure 8. Calculated design capacity compared with experimental shear capacity. Note: *a/d* = shear span–to–depth ratio; M_n = nominal moment capacity. 1 kip = 4.448 kN.

Table 2. Ratios of experimental capacity to predicted capacity

	1965-STD	**ACI**	**AASHTO-SIMP**	**MCFT-EQN**	**MCFT-TAB**
Test A1	0.83	0.88	0.74	1.25	0.98
Test C1	0.95	1.10	0.90	1.25	1.15
Test C2	0.81	0.94	0.77	1.19	0.97
Average	0.86	0.97	0.80	1.23	1.03
COV, %	8.8	11.6	10.7	2.6	9.5

Note: 1965-STD = predicted capacity per the American Association of State Highway Officials' (AASHTO's) *Standard Specifications for Highway Bridges*; ACI = predicted capacity per the American Concrete Institute's *Building Code Requirements for Structural Concrete (ACI 318-14) and Commentary (ACI 318R-14)* shear method; AASHTO-SIMP = predicted capacity per the *AASHTO LRFD Bridge Design Specifications'* simplified procedure; COV = coefficient of variation; MCFT-EQN = predicted capacity per the AASHTO LRFD specifications' modified compression field theory (MCFT) procedure using beta-theta equations; MCFT-TAB = predicted capacity per the AASHTO LRFD specifications' MCFT procedure using beta-theta tables.

methods. The COV was included as an indication of variation for these methods compared with the experimental capacities for the sections tested. The MCFT-EQN method was by far the most conservative, followed by the MCFT-TAB method. The ACI and MCFT-TAB methods provided the most accurate results for the tested configurations. The 1965-STD and AAS-HTO-SIMP methods were generally unconservative for these cases. It is important to note that although this paper primarily compares observed capacities to predicted shear capacities, these failures may not be entirely due to shear, with flexure or bond loss contributing to the failure. Despite this, the capacity equations in the AASHTO LRFD specifications are typically used to rate bridges for shear.

Table 3 shows the various predicted capacities compared with the experimental values using both measured concrete properties and the assumed design properties for the girders. The differences in shear capacities using design or measured properties were small. For load rating, assumed properties are likely adequate.

Finally, two of the failures were categorized as bond shear (A1 and C1). This failure mechanism is not modeled in traditional shear-capacity methods. Recently, a method was developed to account for the effect of loss of strand bond on shear capacity.[18] This procedure was developed based on AASHTO LRFD specifications section 5.8.3.5 for longitudinal rein-

Table 3. Capacities using both measured and design girder properties

	Capacities using measured properties, kip						
Test	1965-STD	ACI	AASHTO-SIMP	MCFT-EQN	MCFT-TAB	Shear at M_n	Actual
A1	191.8	180.9	216.3	128.3	163.0	154.4	160.0
A2	185.9	180.9	207.6	136.0	155.7	187.0	203.0
C1	214.7	185.3	226.6	163.1	177.8	220.6	204.0
C2	221.9	191.4	233.3	149.9	183.7	177.7	179.0
	Capacities using design properties, kip						
Test	1965-STD	ACI	AASHTO-SIMP	MCFT-EQN	MCFT-TAB	Shear at M_n	Actual
A1	191.8	177.1	215.2	126.9	159.8	152.5	160.0
A2	185.9	177.1	206.4	134.0	152.6	184.6	203.0
C1	214.7	177.5	226.9	161.1	171.1	218.6	204.0
C2	221.9	183.3	232.7	147.3	176.1	176.1	179.0

Note: 1965-STD = predicted capacity per the American Association of State Highway Officials' (AASHTO's) *Standard Specifications for Highway Bridges*; ACI = predicted capacity per the American Concrete Institute's *Building Code Requirements for Structural Concrete (ACI 318-14) and Commentary (ACI 318R-14)* shear method; AASHTO-SIMP = predicted capacity per the *AASHTO LRFD Bridge Design Specifications*' simplified procedure; MCFT-EQN = predicted capacity per the AASHTO LRFD specifications' modified compression field theory (MCFT) procedure using beta-theta equations; MCFT-TAB = predicted capacity per the AASHTO LRFD specifications' MCFT procedure using beta-theta tables; M_n = nominal moment capacity. 1 kip = 4.448 kN.

forcing steel in end regions. The method has been verified experimentally for *a/d* between 1.0 and 4.4. For test A1, the nominal shear capacity for the Ross and Naji method[18] was 198 kip (881 kN). This resulted in a 19.1% error compared with the experimental shear capacity. For test C1, the Ross and Naji method resulted in an expected capacity of 226 kip (1005 kN), an error of 9.7% compared with the experimental shear capacity. In both cases, the estimated capacity exceeded the experimental values. Tests A2 and C2 were not compared with this method because they did not result in bond-shear failures. The accuracy of the Ross and Naji method (14% average error) resulted in less error for tests A1 and C1 than the AASHTO-SIMP (18% error) and MCFT-EQN (25% error). Alternatively, the MCFT-TAB method resulted in an error of only 8%, so despite the bond-shear issues it was still the preferred method for the configurations tested.

Experimental capacities compared with demands

Experimental capacities were also compared with the factored demands from the AASHTO LRFD specifications[3] (**Fig. 9**). The lines in the figures represent the demands on an interior and exterior girder of the given bridge (I244A or I244C) using AASHTO LRFD specifications shear-distribution factors. The live-load (LL) shear demands include an impact factor (1.33 × design truck shear) and load factor (strength I factor of 1.75 × LL shear demand). The dead load from the self-weight of the specimens is not included, but the additional dead load related to the tributary-width deck that was not a part of the specimen was factored and added to the total demand. The experimental capacities are not modified by any strength reductions, but

these capacities are much higher than the corresponding demands for the four cases tested. On average, the factored LL demands were 51% of the experimental capacity for interior girders and 60% of the capacity for exterior girders.

Table 4 compares the maximum applied shears from the girder tests $V_{max,exp}$ with the AASHTO LRFD specifications' demands, and the experimental rating factor that would correspond to this level of shear. The AASHTO LRFD specifications' demand is the unfactored demand on the girder based on HL-93 live loads and dead loads due to the tributary width of the deck at the given location. The so-called experimental rating factor is $V_{max,exp}$ divided by the HL-93 shear demand. This is similar to a rating factor for the bridge without any probabilistic factors included. Based on the AASHTO LRFD specifications' distribution factors and demands, the shear demands on these bridges would have to increase greatly to achieve the same amount of shear witnessed in the girder tests. These factors provide an idea of the factor of safety of the bridges under the HL-93 load with respect to the applied shears in all full-scale tests (with no impact or load factors included).

Another question raised from the full-scale tests was the bearing issue reported in test C1. Bearing damage was observed between 90 and 110 kip (400 and 489 kN) of load, corresponding to a 55 to 68 kip (245 to 302 kN) shear at the support. In the I-244 span from which I244C was taken, this level of shear is exceeded by unfactored demands based on the HL-93 load. It is therefore possible that these common levels of corrosion and traffic loads can cause concrete to spall at the ends, revealing more reinforcing steel to harmful environmental conditions. This is a serviceability concern for
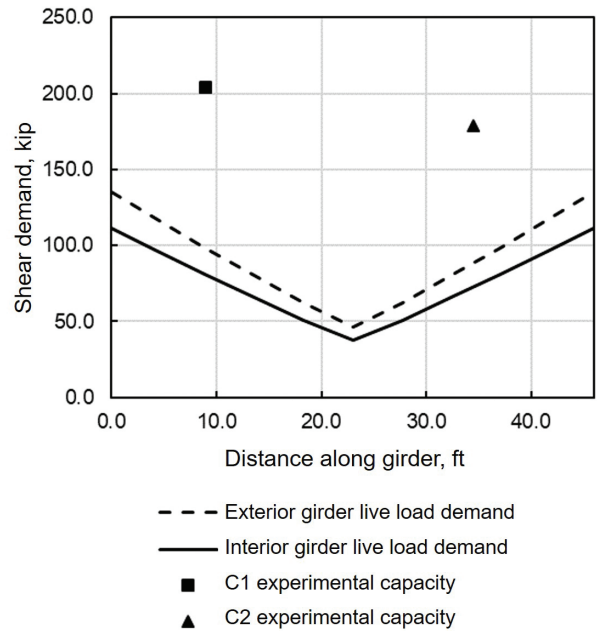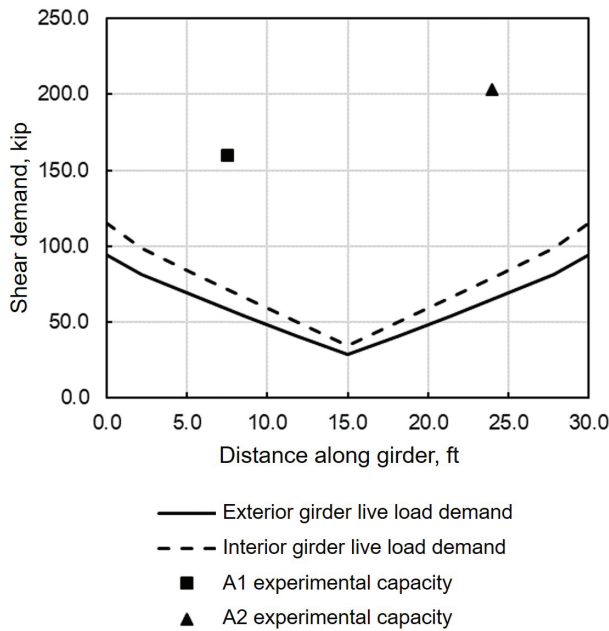
Figure 9. Experimental capacities compared with factored live load shear demand for I244A (left) and I244C (right). Note: 1 ft = 0.305 m; 1 kip = 4.448 kN.

Table 4. Maximum applied shear in full-scale tests compared with unfactored shear demand in bridge

Tested girder	A1		A2		C1		C2	
$V_{max,exp}$, kip	160		203		204		179	
Girder location	Interior	Exterior	Interior	Exterior	Interior	Exterior	Interior	Exterior
Shear distribution factor*	0.791	0.649	0.791	0.649	0.791	0.649	0.791	0.649
Unfactored demand, kip*	33.7	27.7	37.5	30.8	46.0	37.8	41.3	33.9
Experimental rating factor	5.39	6.57	5.41	6.59	4.91	5.98	4.76	5.80

* The shear distribution factors and the unfactored shear demand were calculated per the American Association of State Highway and Transportation Officials' *AASHTO LRFD Bridge Design Specifications*.

Note: $V_{max,exp}$ = maximum shear applied during test. 1 kip = 4.448 kN.

older bridges, especially for longer spans where reactions are larger. Girders with cracking at the ends should be monitored closely in case cracking increases dramatically in service. Despite this damage due to corrosion cracking at the ends, the girders tested were still capable of reaching the capacities calculated by either strain compatibility or MCFT.

Effects of corrosion on shear capacity

When the girders were received, they had visible corrosion of the prestressing strands at the ends of the girders that were similar to what is commonly seen in bridges constructed in the 1960s and 1970s[19] in Oklahoma. Because the girders described in this paper came from an urban area, they were occasionally exposed to deicing chemicals. One goal for the

full-scale tests was to evaluate the effects of this end-region corrosion on shear and bond behavior in these girders. As noted, strand slip was measured in two of the full-scale tests, A1 and C1. These tests were categorized as bond-shear-type failures. In the other tests (A2 and C2), the transfer- and development-length behavior of the strands was not an issue. Therefore, it appears that the corrosion had no effect on the flexural or shear strengths. In tests A1 and C1, it is possible that cracking caused by corrosion at the ends affected the anchorage behavior of the strands. During both tests A1 and C1, flexure-shear cracking entered the development length and led to strand slip and horizontal cracking in the bottom flange, which is indicative of loss of bond. Once bond is lost, either the shear capacity of the section is reduced or load must be carried in a different way.

Load-versus-deflection data were not available for test A1 due to a data acquisition error, but from visual observation during the test, there appeared to be sufficient ductility even after the strands slipped. A large amount of shear cracking occurred throughout the test. Comparing the experimental capacity with the design-estimated capacities gave conflicting results. The 1965 AASHO specifications' equations overestimated the shear capacity, as did the ACI 318 and AASHTO LRFD specifications' simplified procedures. Alternatively, the section reached its full flexural capacity, and the MCFT methods were conservative with regard to shear strength. MCFT appeared to be the most accurate method surveyed for test A1, and it has been shown to be accurate for a wide variety of concrete sections.[20] Because of the section's adequacy based on MCFT and strain compatibility for flexure, the capacity of the section appears to be relatively unaffected by the corrosion at the end, even if it may have affected the failure mechanism (bond shear).

Test C1 was the other load test where strand slip was measured. Cracking due to corrosion was somewhat severe at this end, and at early load steps, preexisting cracks affected the bearing of the girder, causing increased cracking and spalling of concrete. This damage is a serious serviceability issue. Despite these bearing issues, the ultimate capacity appeared relatively unaffected by corrosion and bearing damage. Ductile load-deflection behavior was observed (Fig. 6), though there is not a region of plastic deformation typical of a flexural failure. When the measured capacity and the estimated capacities are compared, the shear-capacity methods were generally more conservative compared with test A1. The 1965 AASHO specifications' and AASHTO LRFD specifications' simplified shear methods overestimated capacity. Unlike test A1, the section did not reach its full flexural capacity as calculated by strain compatibility. In this case, the AASHTO LRFD specifications' simplified method was not a conservative method for calculating the capacity. Similar to test A1, the MCFT methods both produced conservative estimates for test C1. It is recommended that engineers making capacity estimations for older girders use either of the more conservative MCFT methods, especially the MCFT-TAB method.

Behavior of deck during shear tests

Another interesting aspect of this research was the behavior of the composite deck during the tests. Test C2 seems to show that the composite deck, if designed correctly, is capable of carrying a large amount of compression force, as evidenced by buckling of the steel during this test. Strain gauges confirmed that the strain carried by the deck decreases farther from the load point due to shear lag in the deck, as expected. A common finding in all tests was the failure of the deck overlay. In older decks where the driving surface has been replaced with an overlay, the ultimate capacity of the compression zone will be limited by this overlay. Failures observed during this research all included delamination of this surface. The deck overlay was always the last component to fail and was a limiting factor in the ultimate capacity of the girders.

Conclusion

Load tests were performed on two AASHTO Type II girders with different prestressing forces and amounts of the original deck and diaphragms left intact. The test locations were chosen to explore the shear performance from the quarter point to two girder depths from the end (to focus on beam-region shear). Of particular interest in these tests was the age of the girders, corrosion at both ends of each girder, and whether this corrosion affected the performance. The tested girders had varying levels of corrosion at the ends, from moderate to minor. Overall, the girders performed well despite their being in service for more than 45 years. Regarding the ultimate capacities and qualitative performance, the girders generally exceeded predicted capacities and their failures were characterized by significant deflection and shear and flexural cracking. The main conclusions from the girder tests are as follows:

- Experimental values were greater than the calculated capacities when the AASHTO LRFD specifications' MCFT shear methodologies (beta-theta equations or tables) or flexural capacity by strain compatibility were used. The beta-theta equations were the most conservative estimators of shear strength for the configurations tested (average experimental capacity/predicted capacity = 1.23). The experimental capacities of the girders also exceeded their calculated design demands.

- The 1965 AASHO specifications resulted in overprediction of shear strength compared with the experimental values. The AASHTO LRFD specifications' simplified method also yielded larger capacities than those observed experimentally in some cases. Alternatively, the ACI 318 shear method was reasonably accurate (average experimental capacity/predicted capacity = 0.97) and more conservative than the AASHTO LRFD specifications' simplified method (average experimental capacity/predicted capacity = 0.8) for the locations tested.

- Strand slip was observed in two tests and was considered to lead to shear failures. The slip is potentially related to corrosion at the ends, but the loss in bond did not result in an underestimation of ultimate capacity. Despite slip, the MCFT method predicted shear capacity conservatively. Slip did not lead to sudden shear failures.

- Deck overlays on the girders were the last part of the sections to fail and limited the ultimate capacity in every test.

While shear capacities did not appear to be negatively influenced by corrosion, the presence of cracking due to corrosion caused bearing issues at loads that are likely to be seen in service. This potential for cracking could be a serviceability issue for girders with similar levels of damage. This research revealed that unfactored shear demands for bridges of this type were large enough to cause additional damage to corroded girder ends, thereby increasing durability issues.

Acknowledgments

References

1. American Association of State Highway Officials (AASHO). 1965. *Standard Specifications for Highway Bridges*. 9th ed. Washington, DC: AASHO.

2. Murray, C. D., B. N. Cranor, R. W. Floyd, and J.-S. Pei. "Shear Behavior of 45-Year-Old AASHTO Type II Bridge Girders." Paper 57 presented at the 2017 PCI Convention and National Bridge Conference at The Precast Show, Cleveland, OH.

3. American Association of State Highway and Transportation Officials (AASHTO). 2015. *AASHTO LRFD Bridge Design Specifications*. 7th ed. Washington, DC: AASHTO.

4. Shenoy, C. V., and G. C. Frantz. 1991. "Structural Tests of 27-Year-Old Prestressed Concrete Bridge Beams." *PCI Journal* 36 (5): 80–90.

5. Halsey, J. T., and R. Miller. 1996. "Destructive Testing of Two Forty-Year-Old Prestressed Concrete Bridge Beams." *PCI Journal* 41 (5): 84–93.

6. Pessiki, S., M. Kaczinski, and H. H. Wescott. 1996. "Evaluation of Effective Prestress Force in 28-Year-Old Prestressed Concrete Bridge Beams." *PCI Journal* 41 (6): 78–89.

7. Runzell, B., C. Shield, and C. French. 2007. *Shear Capacity of Prestressed Concrete Beams*. Research report MN/RC 2007-47. St. Paul, MN: Minnesota Department of Transportation.

8. ACI (American Concrete Institute) Committee 318. 2014. *Building Code Requirements for Structural Concrete (ACI 318-14) and Commentary (ACI 318R-14)*. Farmington Hills, MI: ACI.

9. Ross, B. E., M. H. Ansley, and H. R. Hamilton III. 2011. "Load Testing of 30-Year-Old AASHTO Type III Highway Bridge Girders." *PCI Journal* 56 (4): 152–163.

10. Hamilton, H. R. III, G. Llanos, and B. E. Ross. 2009. *Shear Performance of Existing Prestressed Concrete Bridge Girders*. Report BD 545-56. Gainesville, FL: University of Florida Department of Civil and Coastal Engineering.

11. Osborn, G. P., P. J. Barr, D. A. Petty, M. W. Halling, and T. R. Brackus. 2012. "Residual Prestress Forces and Shear Capacity of Salvaged Prestressed Concrete Bridge Girders." *Journal of Bridge Engineering* 17 (2): 302–309.

12. Martin, R. D., T. H.-K. Kang, and J.-S. Pei. 2011. "Experimental and Code Analyses for Shear Design of AASHTO Prestressed Concrete Girders." *PCI Journal* 56 (1): 54–74.

13. ACI Committee 214. 2003. *214.4R-10 Guide for Obtaining Cores and Interpreting Compressive Strength Results*. Farmington Hills, MI: ACI.

14. ASTM Subcommittee C09.61. 2014. *Standard Test Method for Static Modulus of Elasticity and Poisson's Ratio of Concrete in Compression*. ASTM C469/C469M-14. West Conshohocken, PA: ASTM International.

15. ASTM Subcommittee A01.05. 2016. *Standard Test Methods for Testing Multi-wire Steel Prestressing Strand*. ASTM A1061/A1061M-16. West Conshohocken, PA: ASTM International.

16. Naji, B., B. E. Ross, and R. W. Floyd. 2017. "Characterization of Bond-Loss Failures in Pretensioned Concrete Girders." *Journal of Bridge Engineering* 22 (4). https://doi.org/10.1061/(ASCE)BE.1943-5592.0001025.

17. Bentz, E. C., F. J. Vecchio, and M. P. Collins. 2006. "Simplified Modified Compression Field Theory for Calculating Shear Strength of Reinforced Concrete Elements." *ACI Structural Journal* 103 (4): 614–624.

18. Ross, B. E., and B. Naji. 2014. "Model for Nominal Bond-Shear Capacity of Pretensioned Concrete Girders." *Transportation Research Record*, no. 2406: 79–86.

19. Mayhorn, D. T. 2016. "Investigation of the Effects of End Region Deterioration in Precast, Prestressed Concrete Bridge Girders." MS thesis, University of Oklahoma, Norman, OK.

20. Vecchio, F. J., and M. P. Collins. 1986. "The Modified Compression-Field Theory for Reinforced Concrete Elements Subjected to Shear." *Journal of the American Concrete Institute* 83 (2): 219–231.

21. Dymond, B. Z., C. E. French, and C. K. Shield. 2016. *Investigation of Shear Distribution Factors in Prestressed Concrete Girder Bridges*. Research report MN/RC 2016-32. St. Paul, MN: Minnesota Department of Transportation.

Notation

a/d = shear span–to–depth ratio

$M_{cracking}$ = applied moment at cracking load

M_{max} = applied moment at maximum load

M_n = nominal moment capacity

M_{slip} = applied moment at first measured strand slip

$P_{cracking}$ = cracking load

P_{max} = maximum load

P_{slip} = load at first measured strand slip

$V_{cracking}$ = applied shear at cracking load

V_{max} = applied shear at maximum load

$V_{max,exp}$ = maximum shear applied during test

V_{slip} = applied shear at first measured strand slip

About the authors

Cameron D. Murray, PhD, is an assistant professor in the Department of Civil Engineering at the University of Arkansas in Fayetteville. His research interests include prestressed concrete, alkali-silica reaction, and rapid-setting concrete.

Brittany N. Cranor is a structural engineer in the Engineering and Construction Design Division of the United States Army Corps of Engineers, Tulsa District. She received her MS in civil engineering in 2015 at the University of Oklahoma in Norman.

Royce W. Floyd, PhD, PE, is an associate professor in the School of Civil Engineering and Environmental Science at the University of Oklahoma in Norman. His research interests include prestressed concrete, lightweight self-consolidating concrete, and rapid-setting concrete.

Jin-Song Pei, PhD, is an associate professor in the School of Civil Engineering and Environmental Science at the University of Oklahoma in Norman. Her research interests include numerical modeling and neural networks.

Abstract

Prestressed concrete bridges designed under previous versions of the American Association of State Highway and Transportation Officials' (AASHTO's) *Standard Specifications for Highway Bridges* have the potential to be inadequate for shear compared with those designed under the *AASHTO LRFD Bridge Design Specifications* due to differences in the ways that the demand side of the shear-strength equation is calculated.

Two approximately 45-year-old AASHTO Type II bridge girders taken from the Interstate 244 bridge over the Arkansas River in Tulsa, Okla., were subjected to a series of nondestructive flexural tests and final destructive tests in order to assess behavior characteristics of aged prestressed concrete members. Shear capacity was predicted based on the original design specifications, the AASHTO LRFD specifications, and methods proposed by other researchers. Of particular interest was the corrosion to the prestressing strands at the ends of the girders. Measured capacities exceeded the predicted values based on modified compression field theory or moment capacity in all cases, but deterioration near the girder ends was observed to influence the failure mechanisms. Factored demands were also exceeded by experimental capacities.

Keywords

Bridge, capacity, demand, girder, rating, shear.

Review policy

This paper was reviewed in accordance with the Precast/Prestressed Concrete Institute's peer-review process.

Reader comments

Please address any reader comments to *PCI Journal* editor-in-chief Emily Lorenz at elorenz@pci.org or Precast/Prestressed Concrete Institute, c/o *PCI Journal*, 200 W. Adams St., Suite 2100, Chicago, IL 60606.